

Photocatalytic activities of N doped TiO₂ coatings on 316L stainless steel by plasma surface alloying technique

WANG He-feng¹, SHU Xue-feng¹, LI Xiu-yan², TANG Bin³

1. Institute of Applied Mechanics and Biomedical Engineering,
Taiyuan University of Technology, Taiyuan 030024, China;

2. Department of Physics and Optoelectronics, Taiyuan University of Technology, Taiyuan 030024, China;

3. Surface Engineering Institute, Taiyuan University of Technology, Taiyuan 030024, China

Received 9 July 2012; accepted 23 August 2012

Abstract: Nitrogen doped titanium dioxide (N-TiO₂) coatings were fabricated by oxidation of the TiN_x coatings in air. TiN_x coatings were prepared on stainless steel (SS) substrates by plasma surface alloying technique. The reference TiO₂ sample was also deposited by oxidation of the Ti coatings in air. The as-prepared coatings were characterized by X-ray diffraction (XRD), X-ray photoelectron spectroscopy (XPS), scanning electron microscopy (SEM) and ultra violet-visible absorption spectroscopy (UV-Vis). The formation of anatase type TiO₂ is confirmed by XRD. SEM measurement indicates a rough surface morphology with sharp, protruding modules after annealing treatment. The band gap of the N-doped sample is reduced from 3.25 eV to 3.08 eV compared with the undoped one. All the N-doped samples show red shift in photoresponse towards visible region and improved photocurrent density under visible irradiance is observed for the N-doped samples. The photocatalytic activity was evaluated via the photocatalytic oxidation of methylene blue (MB) in aqueous under visible light irradiation. The results reveal that the N-doped samples extend the light absorption spectrum toward the visible region. The degradation rate of N-TiO₂ is 20% in visible irradiation for 150 min.

Key words: TiO₂; N doping; photocatalysis; stainless steel; plasma alloying

1 Introduction

Stainless steel (SS) can be used in hospitals, public, food industries and kitchen appliances [1,2]. The existing and breeding of microorganism on the surface of SS products do not meet health criteria. With sustainable improvement of the people's living level, public awareness on safety during food and medicine processing has been rapidly raised. It is crucial to improve the antibacterial properties of SS. One of the promising routes to this end is to deposit a protective ceramic coating on the metal surface. For example, medical metals were coated with silver or copper, which are strong antibacterial metal elements [3–5].

There were many studies trying to prepare antibacterial stainless steel surfaces by coating, ion implantation, chemical synthesis process, etc. [6–8]. However, the surface modifications would fail in a short

time due to dropping off of the antibacterial coatings and then would not provide enough antibacterial functions during utilizations of these coatings. Meanwhile, it is difficult to maintain antibacterial effect simultaneously with good wear and corrosion resistance. Therefore, how to enhance the antibacterial capability of the stainless steel surface and not influence its base performance degradation is needed.

TiO₂, a well known biomaterial, has potential applications including as an antibacterial coating for sterilizing biomedical metallic implants, hospital equipments and as self-cleaning surfaces for use in architecture [9,10]. At the same time, TiO₂ possesses low friction, high wear resistance, excellent corrosion resistance and good biocompatibility [11,12]. However, TiO₂ can only be activated by irradiating with ultraviolet (UV) light due to its high band-gap energies. Therefore, the modification of TiO₂ to render its sensitivity to visible-light became one of the most important goals to

Foundation item: Projects (51171125, 11172195) supported by the National Natural Science Foundation of China; Project (20110321051) supported by the Shanxi Province Programs for Science and Technology Development, China; Project (2011-038) supported by the Shanxi Province Foundation for Returned Overseas Scholars, China; Project (2010081016) supported by the International Scientific and Technological Cooperation Foundation of Shanxi Province, China

Corresponding author: SHU Xue-feng; Tel: +86-351-6010540; +86-13834600938; E-mail: shuxuefengtyut@163.com

increase the utility of TiO₂. For this purpose, doping or combining TiO₂ with various metal or non-metal ions has been considered [13,14]. The TiO₂ doped with non-metals has drawn great attention due to their nontoxic feature. Many attempts have been made in the direction of N, C, or anion-doped TiO₂ photocatalysis because it has good potential for the utilization of solar energy [15–18]. Since ASAMI et al [16] reported that N-doping significantly improved the photocatalytic reactivity of TiO₂ films toward organic molecules under visible light illumination. The most feasible and successful approach among these anions seems to be N-doping.

Recently, many investigations have been made to prepare N-doped TiO₂ coatings by oxidation of TiN_x [19–21], such as anodic oxidation of titanium nitride films prepared by electrophoretic deposition (EPD) [19], oxidation of TiN_x films deposited by reactive DC magnetron sputtering [20]. These show that oxidation of TiN_x films is a viable method to prepare N-doped TiO₂. The plasma surface alloying technique [22,23] is an effective and economical method to improve the surface performance of metals or alloys, such as micro-hardness, wear resistance, and oxidation resistance. The advantage of this technique is that a gradient diffusion layer can be obtained with enough thickness and good adherence between modified layer and the substrate [24].

In principle, N-TiO₂ coatings on metal substrate could be directly obtained by using the plasma surface alloying technique, in which titanium target is sputtered in Ar/O₂/N₂ mixture gas. Two key points should be taken into account. Firstly, oxygen would lead to “target poisoning”, which affects the stability of the process parameters and the deposition rate. Secondly, in glow discharge sputtering, the temperature of the substrate is higher than 800 °C, which would result in the formation of rutile-TiO₂ coatings, rather than the anatase-TiO₂ coatings with good photocatalytic properties.

Based on these considerations, the N-TiO₂ coatings were prepared by two-steps. Firstly, the TiN_x coatings on SS substrate were deposited by plasma surface alloying technique. All the resulted TiN_x coatings were subsequently annealed in air at 450 °C for 2 h to oxidize. The photocatalytic properties of the coatings were measured and discussed by combined theoretical and experimental results.

2 Experimental

2.1 Materials and methods

The 316L SS samples ($d20\text{ mm}\times 5\text{ mm}$) were ground with No. 80–1500 emery papers, and then polished with 0.3 and 0.05 μm alumina powders,

respectively. Finally, the surfaces of samples were cleaned by ethanol and acetone.

The N-TiO₂ coatings were prepared by a two-step processing. Firstly, the TiN_x coatings were deposited on SS substrates by plasma surface alloying technique, in which titanium targets were sputtered in Ar/N₂ mixture gas. The sketch is shown in Fig. 1. The process parameters were as follows: the Ar/N₂ mixture gas pressure was 30–40 Pa ($V(\text{N}_2):V(\text{Ar})=1:2$), the source voltage for supplying Ti elements was –1100 to –550 V, the distance from the source target to the substrate sample was 15 mm, the process temperature was 950 °C and the process duration was 3 h. All the resulted TiN_x coatings were subsequently annealed in air at 450 °C for 2 h to oxidize and crystallize the samples.

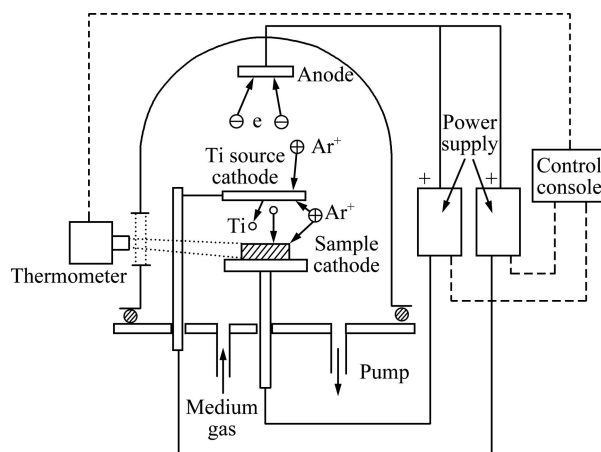


Fig. 1 Sketch of plasma surface alloying technique

2.2 Characterizations

The surface morphologies of the as-deposited and thermally oxidized coatings were examined using scanning electron microscopy (SEM). The composition was determined by X-ray photoelectron spectroscopy (XPS) with Al K α X-ray as the radiation source. An X-ray diffractometer (XRD) with the 1.54 Å Cu K α line as the excitation source was employed to examine the crystal structure of the coatings. The absorption spectra of the samples were collected by UV-Vis spectrophotometer (Shimadzu UV 2450 (Japan)).

2.3 Photocatalytic activity measurement

The surface photocatalytic activity of the samples was measured by photodegradation of MB with the initial concentration and volume of $2.0\times 10^{-5}\text{ mol/L}$ and 30 mL, respectively. First, a piece was settled in aqueous MB in a glass beaker. Then, it was irradiated at room temperature by a halogen lamp (90 W, irradiation distance of 20 cm). The schematic diagram is shown in Fig. 2. It is better to make a visible photocatalyst that works under conventional visible light lamps. The degradation rate was measured by UV-Vis

spectrophotometer at the maximum absorption wavelength of MB. Degradation rate of the solution can be calculated using

$$\eta = \frac{C_0 - C_t}{C_0} \times 100\%$$

where η is the degradation rate, C_0 and C_t are the initial absorbency and the reaction absorbency of MB solution, respectively.

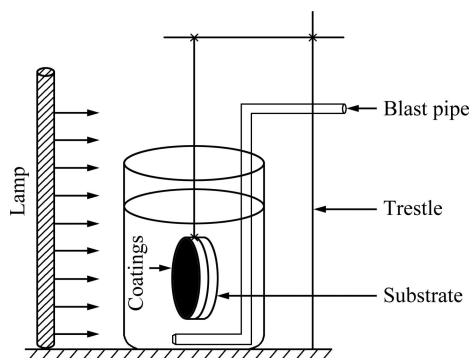


Fig. 2 Schematic diagram of photocatalytic measurement

3 Results and discussion

3.1 XRD

Figure 3 displays the XRD patterns for the undoped sample and N-doped samples before and after annealing. It can be seen from Fig. 3(a) that the as-deposited coatings sputtered under various Ar and N₂ mixture are composed of TiN. The XRD patterns of N-TiO₂ coatings show the characteristic peaks of anatase-TiO₂ (Fig. 3(b)). From the XRD analysis, no characteristic peaks of doping species are detected, and this may be attributed to the fact that the species are present as a highly dispersed state in TiO₂ coatings. Therefore, XPS was also used to analyze the composition of them.

3.2 XPS

To investigate the chemical states of the possible dopants incorporated into TiO₂, N 1s, Ti 2p and O 1s binding energies are studied by measuring the XPS spectra. The results are shown in Fig. 4.

Figure 4(a) shows the chemical binding state of N 1s of the sample. N 1s core level shows a single peak at 400 eV. Recently, in the literature, there has been a controversy about the assignment of N 1s peaks in N-doped TiO₂. ASAH I et al [16] and other authors [25,26] claimed that N can substitute oxygen atoms on the titania surface, producing an XPS-N1s peak localized around 397 eV. Additionally, few nitrogen in the TiO₂ lattice also might reduce the electron density of nitrogen due to the high electronegativity of oxygen and hence a relatively high BE compared to TiN. Indeed SATHISH et al [27]

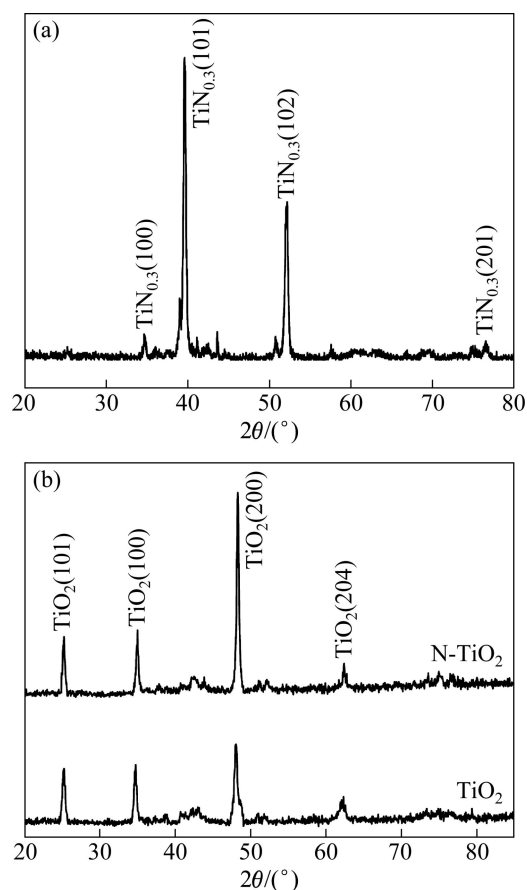


Fig. 3 XRD patterns for undoped sample and N-doped samples before (a) and after (b) annealing

and SIVARANJANI and GOPINATH [28] observed around 398 eV for nanocrystalline N-doped TiO₂ and attributed this to the N—Ti—O environment. This species would be the result of N-doped TiO₂ and visible absorption. However, on the other hand, DIWALD et al [29] and SATHISH et al [27] suggested that the peaks at 399 eV and binding energy higher than 400 eV were due to interstitial N-doping and/or the formation of N—O—Ti species. It might also be due to a different preparation procedure followed by GOLE et al [30].

In this work, we suggest that N-TiO₂ presents interstitial N-doping. Our results on N 1s core levels are consistent with those of RENGIFO-HERRERA et al [31].

The XPS results of Ti 2p are shown in Fig. 4(b). The Ti 2p_{3/2} core levels of the N-TiO₂ is 458 eV, according to other literature and XPS handbook, pure TiO₂ appears at 459 eV [32,33]. While the peak with lower binding energy may be related to the presence of various carbon and nitrogen species, such as Ti—C, Ti—N—O and Ti—O—N [33–36]. This is in agreement with the results as shown in Figs. 4(a) and (b).

Figure 4(c) shows that O 1s peaks appear at 529.3 eV, 531.5 eV and 532.6 eV. The O 1s peak at 529.3 eV is

assigned to the lattice oxygen atom of TiO_2 [37]. The peak at 531.5 eV is related to the oxygen in the surface hydroxyl groups ($-\text{OH}$) and/or in the carbonate species or oxynitrides [37,38]. In addition, the O 1s peak at 532.6 eV is attributed to $\text{C}-\text{O}$ and $\text{C}=\text{O}$ [39].

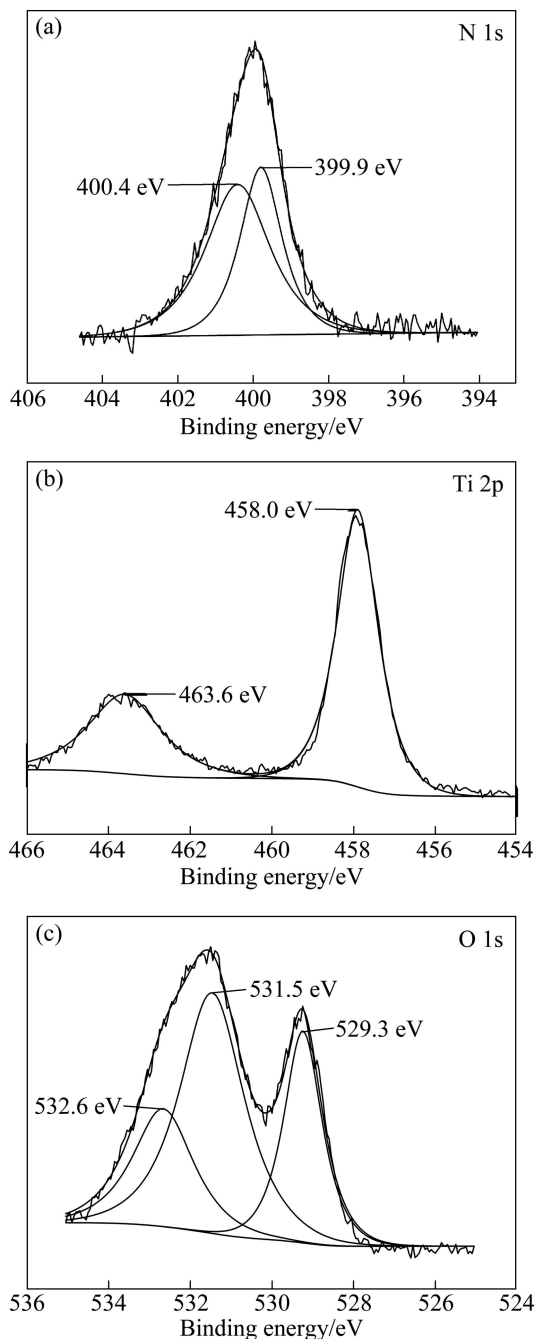


Fig. 4 X-ray photoelectron spectral results collected from N-TiO₂ sample: (a) N 1s; (b) Ti 2p; (c) O 1s

3.3 SEM

Surface morphologies of the undoped sample and N-TiO₂ coated sample are shown in Fig. 5. The surface of the undoped sample exhibits three-dimensional homogenous protuberances growth of grains. Small pinholes are also presented in the coatings (Fig. 5(a)). After thermal oxidation, cracks or pinholes can not be

observed between the grains, and the coatings become denser (Fig. 5(b)). It is noted that the N-TiO₂ coatings have entirely shielded the SS substrates. According to the surface morphology of the calcined coatings, it indicates that thermal oxidation strongly affects the surface morphology.

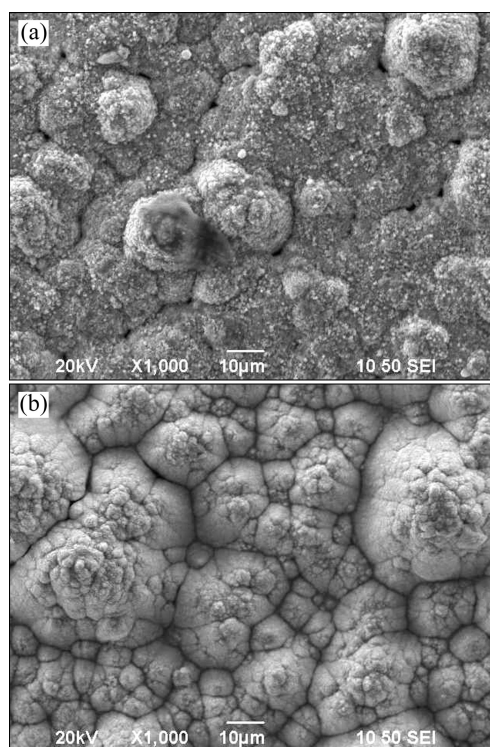


Fig. 5 SEM images of undoped sample (a) and N-doped sample (b)

3.4 UV-vis spectroscopy

The UV-vis absorbance spectra of samples are shown in Fig. 6(a). It can be seen that the N-TiO₂ sample presents a significant absorption in the visible region between 400 and 500 nm, which is the typical absorption feature of nitrogen doped TiO₂ [16,40]. It is clear that the modification of TiO₂ with nitrogen results in the shift of the absorbance region toward longer wavelength, and even into the 500 nm region. The light absorbance of the N-TiO₂ in the visible light region is of great importance for its practical application since it can be activated even by visible light.

Kubelka-Munk function was used to estimate the band gap energy of the prepared samples by plotting $(ah\nu)^{1/2}$ versus energy of light (Fig. 6(b)). The band gap of undoped TiO₂ is 3.25 eV, which is in agreement with other literature values reported for anatase [21,14,41], while that of the N-TiO₂ is obviously decreased from 3.25 eV to 3.08 eV, which indicates that the modification of TiO₂ with nitrogen results in the narrowing of the band gap of TiO₂. This result is mainly attributed to the substitution of the lattice oxygen by nitrogen in the TiO₂ coatings, as can be confirmed by XPS, which results in

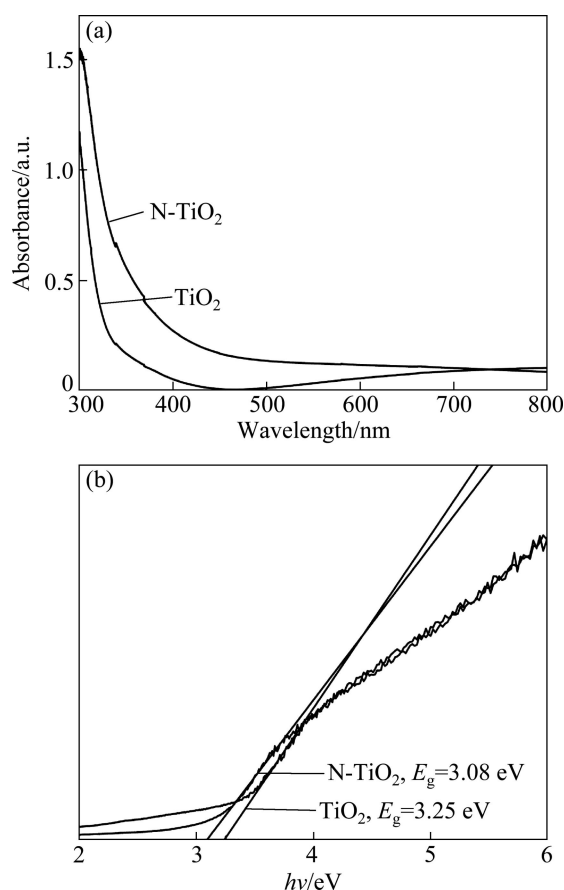


Fig. 6 UV-visible absorption spectra (a) and transformed plots (b) of undoped sample and N-doped sample

the narrow band gap by mixing the N 2p and the O 2p states [16].

3.5 Photocatalytic activity measurements

The photocatalytic degradation of MB under visible light irradiation over N-TiO₂ samples was evaluated and the results are shown in Fig. 7. It is obvious that the N-TiO₂ coatings have higher activity than the pure TiO₂.

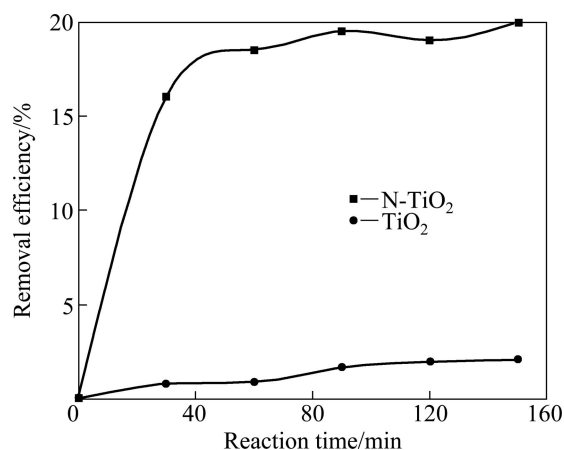


Fig. 7 Photocatalytic degradation of MB using different samples under visible light irradiations

The degradation rates of pure TiO₂ and N-TiO₂ are 2.1% and 20% in visible irradiation for 150 min, respectively. The difference in the photocatalytic activity can be ascribed to additional stronger absorbance in the visible light range by doping with N. Similar results have also been observed for the F or I doping in TiO₂ [42–45]. It is known that the photocatalytic activity of TiO₂ is phase-dependent. Anatase exhibits the highest activity in photocatalysis. Therefore, the higher photocatalytic activity of N-TiO₂ calcined at 450 °C is due to entire anatase phase.

4 Conclusions

N-TiO₂ coatings are prepared by oxidative annealing of sputtered TiN_x coatings. XRD result shows that the crystal structures of N-TiO₂ coated samples are anatase. UV-Vis analysis reveals a red shift on absorption edge toward visible region in N-TiO₂ coatings. Further, the photocatalytic activity of N-TiO₂ coatings demonstrated that by increasing visible light illumination time, the maximum absorption peak and concentration of MB decrease in the presence of N-TiO₂ coatings.

References

- [1] YANG Ke, LÜ Man-qi. Antibacterial properties of an austenitic antibacterial stainless steel and its security for human body [J]. Journal of Materials Science and Technology, 2007, 23(3): 333–336. (in Chinese)
- [2] HONG I T, KOO C H. Antibacterial properties, corrosion resistance and mechanical properties of Cu-modified SUS 304 stainless steel [J]. Materials Science and Engineering A, 2005, 393(1–2): 213–222.
- [3] ZHANG Wei, ZHANG Yi-he, JI Jun-hui, ZHAO Jun, YAN Qing, CHU P K. Antimicrobial properties of copper plasma-modified polyethylene [J]. Polymer, 2006, 47(21): 7441–7445.
- [4] DANIEL A, le PEN C, ARCHAMBEAU C, RENIERS F. Use of a PECVD–PVD process for the deposition of copper containing organosilicon thin films on steel [J]. Applied Surface Science, 2009, 256(3): s82–s85.
- [5] WAN Y Z, RAMAN S, HE F, HUANG Y. Surface modification of medical metals by ion implantation of silver and copper [J]. Vacuum, 2007, 81(9): 1114–1118.
- [6] TIAN X B, WANG Z M, YANG S Q, LUO Z J, RICKY K Y, PAUL F, CHU K. Antibacterial copper-containing titanium nitride films produced by dual magnetron sputtering [J]. Surface and Coatings Technology, 2007, 201(19–20): 8606–8609.
- [7] DAN Z G, NI H W, XU B F, XIONG J, XIONG P Y. Microstructure and antibacterial properties of AISI 420 stainless steel implanted by copper ions [J]. Thin Solid Films, 2005, 492(1–2): 93–100.
- [8] CHEN L M, ZHENG L, LV Y H, LIU H, WANG G C, REN N, LIU D, WANG J Y, BOUGHTON R I. Chemical assembly of silver nanoparticles on stainless steel for antimicrobial applications [J]. Surface and Coatings Technology, 2010, 204(23): 3871–3875.
- [9] RANA S, RAWAT J, SORENSON M M, MISRA R D K. Antimicrobial function of Nd³⁺-doped anatase titania-coated nickel ferrite composite nanoparticles: A biomaterial system [J]. Acta Biomaterialia, 2006, 2(4): 421–432.

- [10] VALLES G, GONZALEZ-MELENDI P, GONZALEZ-CARRASCO J L, SALDANA L, SANCHEZ-SABATE E, MUNUERA L, VILABO A N. Differential inflammatory macrophage response to rutile and titanium particles [J]. *Biomaterials*, 2006, 27(30): 5199–5211.
- [11] KRISHNA D S R, SUN Y, CHEN Z. Magnetron sputtered TiO₂ films on a stainless steel substrate: selective rutile phase formation and its tribological and anti-corrosion performance [J]. *Thin Solid Films*, 2011, 519(15): 4860–4864.
- [12] SHAN C, HOU X, CHOY K. Corrosion resistance of TiO₂ films grown on stainless steel by atomic layer deposition [J]. *Surface and Coatings Technology*, 2008, 202(11): 2399–2402.
- [13] HOFFMANN M R, MARTIN S T, CHOI W, BAHNEMAN D W. Environmental applications of semiconductor photocatalysis [J]. *Chemical Reviews*, 1995, 95(1): 69–95.
- [14] LINSEBIGLER A L, LU G, YATES J T. Photocatalysis on TiO₂ surfaces: principles, mechanisms, and selected results [J]. *Chemical Reviews*, 1995, 95(3): 735–758.
- [15] CUI X L, MA M, ZHANG W, YANG Y C, ZHANG Z J. Nitrogen-doped TiO₂ from TiN and its visible light photoelectrochemical properties [J]. *Electrochemistry Communications*, 2008, 10(3): 367–371.
- [16] ASAH I R, MORIKAWA T, OHWAKI T, AOKI K, TAGA Y. Visible-light photocatalysis in nitrogen-doped titanium oxides [J]. *Science*, 2001, 293(5528): 269–271.
- [17] ZHU Lei, CUI Xiao-li, SHEN Jie, YANG Xi-liang, ZHANG Zhuang-jian. Visible light photoelectrochemical response of carbon-doped TiO₂ thin films prepared by DC reactive magnetron sputtering [J]. *Acta Physico-Chimica Sinica*, 2007, 23(11): 1662–1666. (in Chinese)
- [18] HO W, YU J C, LEE S. Synthesis of hierarchical nanoporous F-doped TiO₂ spheres with visible light photocatalytic activity [J]. *Chemical Communications*, 2006, 22(10): 1115–1117.
- [19] YU Zhi-yong, ZHANG Wei, MA Ming, CUI Xiao-li. Visible light photoelectrochemical response of nitrogen-doped TiO₂ thin films prepared by anodic oxidation of titanium nitride films [J]. *Acta Physico-Chimica Sinica*, 2009, 25(1): 35–40. (in Chinese)
- [20] BRUDNIK A, BUCKO M, RADECKA M, TRENCZEK-ZAJAC A, ZAKRZEWSKA K. Microstructure and optical properties of photoactive TiO₂: N thin films [J]. *Vacuum*, 2008, 82(10): 936–941.
- [21] ORLOV A, TIKHOV M S, LAMBERT R M. Application of surface science techniques in the study of environmental photocatalysis: Nitrogen-doped TiO₂ [J]. *Comptes Rendus Chimie*, 2006, 9(5–6): 794–799.
- [22] XU Z, LIU X, ZHANG P, ZHANG Y, ZHANG G, HE Z. Double glow plasma surface alloying and plasma nitriding [J]. *Surface and Coatings Technology*, 2007, 201 (9–11): 4822–4825.
- [23] CONG W, YAO Z J, ZHU X L. Sliding wear of low carbon steel modified by double-glow plasma surface alloying with nickel and chromium at various temperatures [J]. *Wear*, 2010, 268(5–6): 790–796.
- [24] WANG Z X, HE Z Y, WANG Y Q, LIU X P, TANG B. Microstructure and tribological behaviors of Ti6Al4V alloy treated by plasma Ni alloying [J]. *Applied Surface Science*, 2011, 257(23): 10267–10272.
- [25] NAMBU A, GRACIANI J, RODRIGUEZ J A, WU Q, FUJITA E, FERNANDEZ-SANZ J J. N-doping of TiO₂(110): photoemission and density functional studies [J]. *The Journal of Chemical Physics*, 2006, 125(9): 094706-1–094706-8.
- [26] DIWALD O, THOMPSON T L, GORALSKI E G, WALCK S D, YATES J T. The effect of nitrogen ion implantation on the photoactivity of TiO₂ rutile single crystals [J]. *Journal of Physical Chemistry B*, 2004, 108(1): 52–57.
- [27] SATHISH M, VISWANATHAN B, VISWANATH R P, GOPINATH C S. Synthesis, characterization, electronic structure, and photocatalytic activity of nitrogen-doped TiO₂ nanocatalyst [J]. *Chemistry of materials*, 2005, 17(25): 6349–6353.
- [28] SIVARANJANI K, GOPINATH C S. Porosity driven photocatalytic activity of wormhole mesoporous TiO_{2-x}N_x in direct sunlight [J]. *Journal of Materials Chemistry*, 2011, 21(8): 2639–2647.
- [29] DIWALD O, THOMPSON T L, GORALSKI E G, WALCK S D, YATES J T. Photochemical activity of nitrogen-doped rutile TiO₂(110) in visible light [J]. *Journal of Physical Chemistry B*, 2004, 108(19): 6004–6008.
- [30] GOLE J L, STOUT J D, BURDA C, LOU Y, CHEN X. Highly efficient formation of visible light tunable TiO_{2-x}N_x photocatalysts and their transformation at the nanoscale [J]. *Journal of Physical Chemistry B*, 2004, 108(4): 1230–1240.
- [31] RENGIFO-HERRERA J A, KIWI J, PULGARIN C. N, S co-doped and N-doped Degussa P-25 powders with visible light response prepared by mechanical mixing of thiourea and urea. Reactivity towards *E. coli* inactivation and phenol oxidation [J]. *Journal of Photochemistry and Photobiology A: Chemistry*, 2009, 205(2–3): 109–115.
- [32] MA Y F, ZHANG J L, TIAN B Z, CHEN F, WANG L Z. Synthesis and characterization of thermally stable Sm, N co-doped TiO₂ with highly visible light activity [J]. *Journal of Hazardous Materials*, 2010, 182(1–3): 386–393.
- [33] WANG X, LIM T T. Solvothermal synthesis of C–N codoped TiO₂ and photocatalytic evaluation for bisphenol A degradation using a visible-light irradiated LED photoreactor– [J]. *Applied Catalysis B*, 2010, 100(1–2): 355–364.
- [34] OHNO T, AKIYOSHI M, UMEBAYASHI T, ASAI K, MITSUI T, MATSUMURA M. Preparation of S-doped TiO₂ photocatalysts and their photocatalytic activities under visible light [J]. *Applied Catalysis A*, 2004, 265(1): 115–121.
- [35] CHEN X, BURDA C. Photoelectron spectroscopic investigation of nitrogen-doped titania nanoparticles [J]. *Journal of Physical Chemistry B*, 2004, 108(40): 15446–15449.
- [36] WANG P H, YAP P S, LIM T T. C–N–S tridoped TiO₂ for photocatalytic degradation of tetracycline under visible-light irradiation [J]. *Applied Catalysis A*, 2011, 399(1–2): 252–261.
- [37] GORSKA P, ZALESKA A, KOWALSKA E, KLIMCZUK T, SOBCZAK J W, SKWAREK E, JANUSZ W, HUPKA J. TiO₂ photoactivity in vis and UV light: The influence of calcination temperature and surface properties [J]. *Applied Catalysis B*, 2008, 84(3–4): 440–447.
- [38] CHEN X, LOU Y B, SAMIA A, BURDA C, GOLE J. Formation of oxynitride as the photocatalytic enhancing site in nitrogen-doped titania nanocatalysts: Comparison to a commercial nanopowder [J]. *Advanced Functional Materials*, 2005, 15(1): 41–49.
- [39] JIMENEZ C, BARROS D D, DARRAZ A, DESCHANVRES J L, RAPENNE L, CHAUDOUET P, MENDEZ J E, WEISS F, THOMACHOT M, SINDZINGRE T, BERTHOMEG, FERRER F J. Deposition of TiO₂ thin films by atmospheric plasma post-discharge assisted injection MOCVD [J]. *Surface and Coatings Technology*, 2007, 201(22–23): 8971–8975.
- [40] LINDGREN T, MWABORA J M, AVENDAO E, JONSSON J, HOEL A, GRANQVIST C G, LINDQUIST S E. Photoelectrochemical and optical properties of nitrogen doped titanium dioxide films prepared by reactive DC magnetron sputtering [J]. *Journal of Physical Chemistry B*, 2003, 107(24): 5709–5716.

- [41] SYKES E C H, TIKHOV M S, LAMBERT R M. Surface composition, morphology, and catalytic activity of model polycrystalline titania surfaces [J]. *Journal of Physical Chemistry B*, 2002, 106(29): 7290–7294.
- [42] YU J C, YU J G, HO W K, JIANG Z T, ZHANG L Z. Effects of F⁻ doping on the photocatalytic activity and microstructures of nanocrystalline TiO₂ powders [J]. *Chemistry of materials*, 2002, 14(9): 3808–3816.
- [43] YU J G, YU J C, CHENG B, HARK S K, IU K S J. The effect of F⁻-doping and temperature on the structural and textural evolution of mesoporous TiO₂ powders [J]. *Journal of Solid State Chemistry*, 2003, 174(2): 372–380.
- [44] HONG X T, WANG Z P, CAI W M, LU F, ZHANG J, YANG Y Z, MA N, LIU Y J. Visible-light-activated nanoparticle photocatalyst of iodine-doped titanium dioxide [J]. *Chemistry of Materials*, 2005, 17(6): 1548–1552.
- [45] LIU G, CHEN Z, DONG C, ZHAO Y, LI F, LU G Q, CHENG H M. Visible light photocatalyst: Iodine-doped mesoporous titania with a bicrystalline framework [J]. *Journal of Physical Chemistry B*, 2006, 110(42): 20823–20828.

等离子复合处理制备光催化 N 掺杂 TiO₂ 薄膜

王鹤峰¹, 树学峰¹, 李秀燕², 唐 宾³

1. 太原理工大学 应用力学与生物医学工程研究所, 太原 030024;
2. 太原理工大学 物理与光电工程学院, 太原 030024;
3. 太原理工大学 表面工程研究所, 太原 030024

摘 要: 通过等离子合金化技术在不锈钢表面制备 TiN 薄膜, 然后对 TiN 薄膜进行热氧化得到 N 掺杂 TiO₂ 薄膜。同时制备 TiO₂ 薄膜作为对比研究。利用 X 射线衍射(XRD)、X 射线光电子能谱(XPS)、扫描电子显微镜(SEM)及紫外-可见分光光度计(UV-Vis)对得到的薄膜进行表征。XRD 测试结果表明: 经过 450 °C 氧化处理的薄膜中存在锐钛矿晶型的 TiO₂。经热氧化后薄膜表面均匀分布着尺寸接近的微小凸起物。TiO₂ 和 N 掺杂 TiO₂ 的带隙分别为 3.25 eV 和 3.08 eV。可见光下薄膜催化剂降解亚甲基蓝溶液的实验结果表明: N 掺杂 TiO₂ 薄膜比未掺杂 TiO₂ 薄膜的光催化效率高, 可见光照射 150 min 后对亚甲基蓝溶液的最终降解率为 20%。

关键词: TiO₂; N 掺杂; 光催化; 不锈钢; 等离子表面合金化

(Edited by HE Yun-bin)